2015 The 5th International Workshop on Computer Science and Engineering
doi: 10.18178/wcse.2015.04.058

A New Modeling Approach of Flexible Baseline for Distributed POS

Guo Tao[a], Zhuangsheng Zhu[b]
XueYuan Road No.37,HaiDian District,Beijing,China
[a]bestguotao@163.com, [b]zszhu@buaa.edu.cn

Keywords: Distributed POS, Transfer Alignment, Flexible Baseline, Error Model

Abstract. Currently distributed POS(Position and Orientation System) system has been widely used in all kinds of aerial remote sensing equipment, while transfer alignment is just an important link of distributed POS. In traditional transfer alignment model, flexural deflections of wings are ignored, so that flexural deflection of flexible baseline brought by internal and external interference will be introduced into actual system work. Thus new transfer alignment model must be built, and generally there are three approaches: First, H∞ filtering algorithm with stronger robustness is adopted rather than wings modeling, however, its filtering precision and convergence rate are lower than that of Kalman filtering; Second, transducer are adopted to detect bending deflections of wings, but with the improvement of POS precision, test data provided by PVDF(Polyvinylidene Fluoride) can no longer meet the requirements of measurement; Third, angle observed quantity of flexural deflections are added into Kalman filter formulation, and motion equation of flexible wings is established to estimate and compensate for deformation angles. This modeling method could conclude the structure of aerial carrier, and in this thesis, aeroelasticity is applied to regard wings as cantilever model of Timoshenko type, and it's also added in to filter equation of transfer alignment to make the modeling more flexible. The simulation results show that estimated accuracy of x direction and y direction is very high, error of estimation is less than 3'; estimated accuracy of z direction is lower, the error of estimation is less than 5', the error of flexural deflection angle is less then 1', which shows that installation error angle and flexural deflection could be estimated effectively by using the model established in this thesis.

Introduction

Aerial remote sensing system is the most effective method to obtain high-precision remote sensing data utilizing observation load, taking airplane as observation platform. Typical aerial remote sensing system composes of aircraft, remote sensing load, stabilized platform carrying remote sensing system and measuring system of position posture.

Fundamental of aerial remote sensing imaging requires the aerial carrier to fly straightly at a uniform velocity. But due to influences of atmospheric turbulences and equipment characteristics, there must be effects of disturbing forces along flight direction and side direction of the aerial carrier, and the effects will lead to results that original points of remote sensing equipment deviate from ideal uniform linear translational motion. Hence, in the process of remote sensing imaging, this part of motion errors shall be measured accurately, and compensated during imaging procedures.

Airborne high-resolution InSAR(Interferometric Synthetic Aperture Radar) requires uniform linear motion of the aerial carrier. During imaging process, slight high-frequency motion error leads to complicated grating lobe effects and deterioration of Signal to Noise Ratio (SNR), further result in abrupt degradation of imaging quality of synthetic aperture. Hence, SAR must make motion compensation relying on phase center position and velocity information of POS measuring antenna, thus to realize high-resolution real-time imaging. Therefore, high-precision POS is a necessary measure for airborne microwave imaging load to realize high resolution imaging and high precision interference imaging.

SAR antennas are distributed in different positions on the flying platform, motion information of every antenna shall be precisely measured by POS, and location point of antenna shall be fixed with IMU, so that a distributed multi-node POS system is formed[1]. As shown in figure 1:

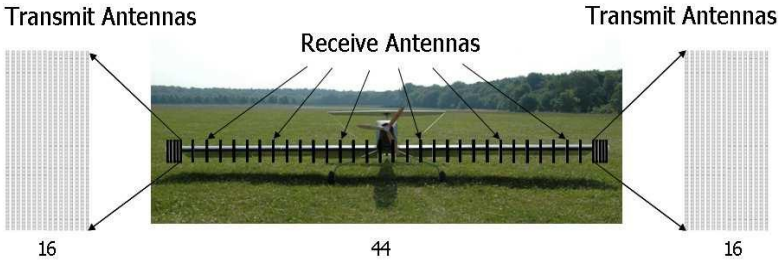

Fig. 1 Schematic figure of distributed POS

However, because aerial carrier is not a perfectly rigid body, during maneuvering flight, airplane will be effected by airflows like turbulence flow, thus to change the shape of the wings. Hence, flexural deflection of wings on aerial carrier are analyzed, researched and compensated, which is helpful to improve measurement accuracy of distributed POS.

Before transfer alignment filtering, we must build vibration model of flexible baseline (wings) to facilitate adding equation to state equation in following Kalman filter, thus to make it convenient to estimate real time vibration characteristics of flexible wings.

Because the vibration of wings could adopt approximate simulation of elastic mechanics characteristics of cantilevers, this thesis includes modeling and analysis for the deformation of cantilevers under outside interferences. During modeling process, cantilevers could be divided into Euler-Bernoulli beam and Timoshenko beam, which are applied under different situations.

Establishment of Timoshenko Model

In the unit of Euler-Bernoulli beam, shear deformation of the beam is ignored[2]. In practical engineering application, situations under which shear deformation shall be considered usually occur. Considering shear deformation, Timoshenko theory could be adopted. For Timoshenko beam, after deformation, sections which are perpendicular to middle surface changed, and rotation angle of sections change to

$$\theta = \frac{dv}{dx} - \gamma \tag{1}$$

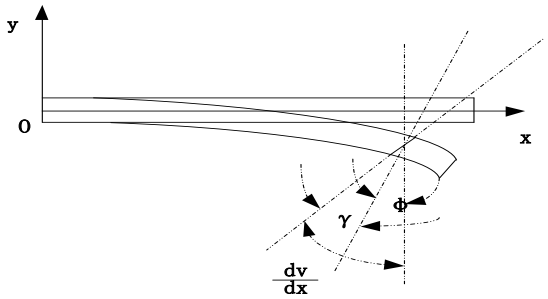

Figure 2 Schematic figure of beam shear deformation

Considering displacement of any section of the beam, there is

$$u(x,y) = -y\theta(x) \tag{2}$$

$$v(x) = v \tag{3}$$

In the equation: u (x, y) is the displacement of beam along axial direction.

From equation (2) and (3), axial strain and shear strain of the beam shall be:

$$\varepsilon = -y\frac{d\theta}{dx} \tag{4}$$

$$\gamma = -\theta + \frac{dv}{dx} \tag{5}$$

Here principle of minimum potential energy is used to deduce matrix equation of the beam[3]. Strain energy of the beam unit is

$$U = \frac{1}{2} b \int_0^l \int_{-h/2}^{h/2} \varepsilon^T E \varepsilon dy dx + \frac{1}{2} b \int_0^l \int_{-h/2}^{h/2} \gamma^T \frac{G}{k} \gamma dy dx \tag{6}$$

In the equation, b, h and l are respectively the width, height and length of the beam, k is introduced as a correction factor for considering actual shear strain and shear stress rather than uniform distribution, for rectangular section k=6/5 is recommendable, while for circular section k=10/9 is advisable.

Substitute equation (4) and (5) into equation (6), we can get

$$U = \frac{1}{2} \int_0^l \left(\frac{d\theta}{dx} \right)^T EI \left(\frac{d\theta}{dx} \right) dx + \frac{1}{2} \int_0^l \left(-\theta + \frac{dv}{dx} \right)^T \frac{GA}{k} \left(-\theta + \frac{dv}{dx} \right) dx \tag{7}$$

Thereinto, $I = \int_{-h/2}^{h/2} by^2 dy$, $A = \int_{-h/2}^{h/2} b dy$ are respectively cross sectional moment of inertia and cross-sectional area of the beam.

In Timoshenko beam unit, lateral displacement v and rotation angle θ are independent, which could be interpolated independently, then we get

$$\mathrm{v} = \begin{bmatrix} N_1 & N_2 \end{bmatrix} \begin{Bmatrix} v_1 \\ v_2 \end{Bmatrix} \tag{8}$$

$$\theta = \begin{bmatrix} N_1 & N_2 \end{bmatrix} \begin{Bmatrix} \theta_1 \\ \theta_2 \end{Bmatrix} \tag{9}$$

In this equation, N_1 and N_2 are linear functions.

$$N_1 = \frac{1}{2}(1-\xi), N_2 = \frac{1}{2}(1+\xi) \tag{10}$$

Substitute equation (8) and equation (9) into the expression of strain energy (7), we can get

$$\frac{1}{2} \int_0^l \left(-\theta + \frac{dv}{dx} \right)^T \frac{GA}{k} \left(-\theta + \frac{dv}{dx} \right) dx = \frac{1}{2} \delta^{eT} \boldsymbol{K}_s^e \delta^e \tag{11}$$

It can be seen that stiffness matrix of Timoshenko beam unit is:

$$\boldsymbol{K}^e = \boldsymbol{K}_b^e + \boldsymbol{K}_s^e \tag{12}$$

Mass matrix of Timoshenko beam could be obtained by kinetic energy expression. Kinetic energy of the unit could be expressed as

$$T = \frac{1}{2} \int_0^l \int_{-h/2}^{h/2} v^T \rho v dy dx = \frac{1}{2} \int_0^l v^T \rho A \dot{v} dx \tag{13}$$

In this equation, ρ is mass density of the unit[4].

Substitute equation (8) into equation (13), we can get

$$T = \frac{1}{2} \delta^{eT} \boldsymbol{M}^e \dot{\delta}^e \tag{14}$$

Thus element mass matrix of Timoshenko is

$$\boldsymbol{M}^e = \int_0^l \boldsymbol{N}^T \rho A \boldsymbol{N} dx = \frac{\rho A l}{6} \begin{bmatrix} 2 & 0 & 1 & 0 \\ 0 & 0 & 0 & 0 \\ 1 & 0 & 2 & 0 \\ 0 & 0 & 0 & 0 \end{bmatrix} \tag{15}$$

After construction of element matrix and vector quantity, matrix equation of beam structure is

$$\boldsymbol{M}\ddot{\delta} + \boldsymbol{K}\delta = \boldsymbol{F}(t) \tag{16}$$

Above equation is named as system equation of motion of beam structure. Solve this equation, we can get dynamic response of the beam.

Establishment of transfer alignment model

Establishment of state equation

In this thesis Kalman filter simulation refers that navigation parameters of main POS is supposed to be accurate to simulate error parameters of slave POS, so that GPS combined parameters are ignored temporarily, and in reality modeling combined navigation results of main POS are required to carry out transfer alignment to slave POS[5]. Specific error models are as follows:

$$\begin{cases} \dot{\boldsymbol{\phi}}^t = \delta\boldsymbol{\omega}_{ie}^t + \delta\boldsymbol{\omega}_{et}^t - (\boldsymbol{\omega}_{ie}^t + \boldsymbol{\omega}_{et}^t) \times \boldsymbol{\phi}^t + \boldsymbol{\varepsilon}^b \\ \delta\dot{\boldsymbol{V}}^t = \delta \boldsymbol{f}^t - (2\delta\boldsymbol{\omega}_{ie}^t + \delta\boldsymbol{\omega}_{et}^t) \times \boldsymbol{V}^t - (2\boldsymbol{\omega}_{ie}^t + \boldsymbol{\omega}_{et}^t) \times \delta\boldsymbol{V}^t + \delta\boldsymbol{g}^t \\ \dot{\boldsymbol{\varepsilon}}^b = 0 \\ \dot{\nabla}^b = 0 \\ \dot{\boldsymbol{\lambda}} = 0 \\ \ddot{\mu}_y(l,t) = -\dot{\psi}_1(l) w_{q1} \mu_y(l,t) - 2\dot{\psi}_1(l) \xi_{q1} w_{q1} \dot{\mu}_y(l,t) + f_{q1} \end{cases} \tag{17}$$

Thereinto $\boldsymbol{\phi}^t$ is misystem relative to inertial coordinate system; $^{\delta}\boldsymbol{\omega}_{et}^t$ is angular velocity error of geographic coordinate system relative to terrestrial coordinate system; $\boldsymbol{\varepsilon}^b$ is drifting of gyroscope; $\delta\dot{\boldsymbol{V}}^t$ is velocity error between main and slave POS; $\delta \boldsymbol{f}^t$ is measurement specific force between main and slave POS; $\delta\boldsymbol{g}^t$ is the error of gsalignment angle of inertial navigation system; $^{\delta}\boldsymbol{\omega}_{\mathrm{ie}}^t$ is angular velocity error of terrestrial coordinate ravitational acceleration; ∇^b is constant bias of accelerometer; $\boldsymbol{\lambda}$ is fix error angle. System state equation is:

$$\dot{\boldsymbol{X}} = \boldsymbol{F}\boldsymbol{X} + \boldsymbol{G}\boldsymbol{W} \tag{18}$$

In this equation:

$$X = \begin{bmatrix} \phi^n & \delta V^n & \varepsilon^b & \nabla^b & \lambda & \mu_y & \dot{\mu}_y \end{bmatrix}^T;\ \phi^t = \begin{bmatrix} \phi_x & \phi_y & \phi_z \end{bmatrix}^T;$$

$$\delta V^t = \begin{bmatrix} \delta V_x & \delta V_y \end{bmatrix}^T;\ \varepsilon^b = \begin{bmatrix} \varepsilon_x^b & \varepsilon_y^b & \varepsilon_z^b \end{bmatrix}^T;\ \nabla^b = \begin{bmatrix} \nabla_x^b & \nabla_y^b \end{bmatrix}^T;$$

$$\lambda = \begin{bmatrix} \lambda_x & \lambda_y & \lambda_z \end{bmatrix}^T;$$

W is systematic noise, G is noise distribution matrix[6], details are as follows:

$$G = \begin{bmatrix} G_1 & 0_{3\times2} & 0_{3\times1} \\ 0_{2\times3} & I_{2\times2} & 0_{2\times1} \\ 0_{10\times3} & 0_{10\times2} & G_2 \end{bmatrix}_{15\times6}$$

, thereinto: $G_1 = C_b^t$, $G_2 = \begin{bmatrix} 0 & 0 & 0 & 0 & 0 & 0 & 0 & 0 & 0 & 1 \end{bmatrix}_{10\times1}^T$.

3.2 Establishment of measurement equation

This thesis adopts the matching mode of velocity + orientation, so that there are 5 measuration quantities, which respectively are attitude angles differences of 3 main and slave POS, and velocity differences of 2 main and slave POS[7]. Details are as follows:

$$Z = HX + V \tag{19}$$

Thereinto H is measuration matrix, $\boldsymbol{H} = \begin{bmatrix} \boldsymbol{H}_1 & \boldsymbol{0}_{3\times3} & \boldsymbol{0}_{3\times3} & \boldsymbol{0}_{3\times3} & \boldsymbol{H}_2 & \boldsymbol{H}_3 & \boldsymbol{0}_{3\times1} \\ \boldsymbol{0}_{2\times3} & \boldsymbol{I}_{2\times2} & \boldsymbol{0}_{2\times3} & \boldsymbol{0}_{2\times2} & \boldsymbol{0}_{2\times3} & \boldsymbol{0}_{2\times1} & \boldsymbol{0}_{2\times1} \end{bmatrix}_{5\times15}$.

4. Analysis of simulation result

4.1Simulation conditions and parameters

POS data adopted in this thesis is U type trajectory data, whose course angle changes 180 degrees in all, and flight speed is 100m/s. Figure 3 is the track of simulation.

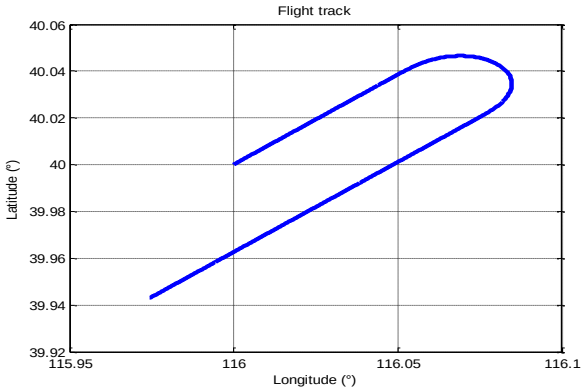

Fig. 3. The flight track for the simulation

Flight parameters: flight height is 3000m; initial longitude 116; initial latitude is 40; initial velocity is 0; initial pitching angle, roll angle and course angle are [0 °0 °45 °].

Device parameters: random drift of gyroscope is 0.01 °/h; constant drift of gyroscope is 0.02 °/h; random error of accelerometer is 50ug; constant bias of accelerometer is 100ug.

4.2 Simulation results

Evaluated error of fix error angle is shown in figure 4:

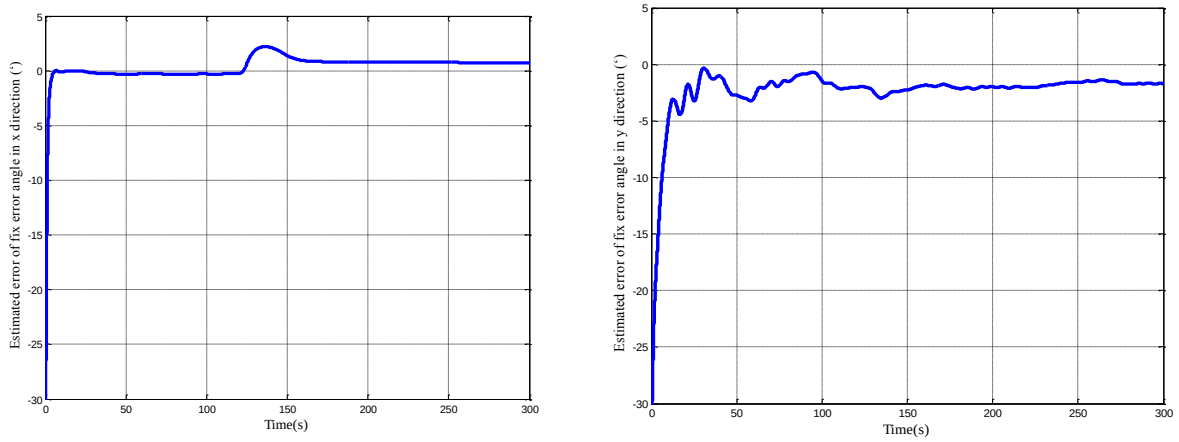

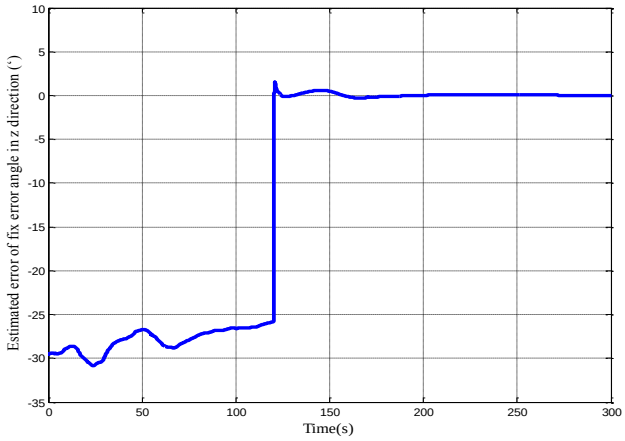

Fig. 4. Evaluated error of fix error angle

Estimated value and estimated error of flexural deflection angle about y axis are shown in Fig. 5:

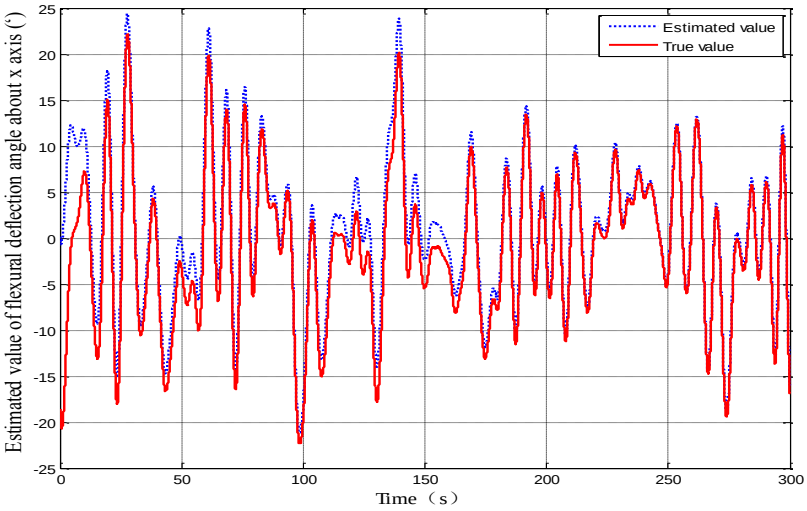

Fig. 5 Estimated value of flexural deflection angle about x axis

From simulation results we can see that U type turning maneuver could improve estimated precision and convergence rate of fix error angle. After U type turning, estimated error of fix error angles of three directions and flexural deflection angle converge. After swing of side rolling, statistical information of estimated value of attitude error between main and slave POS is show in table 1.

Table 1: Statistical property after U type turning

		Error angle in x direction(')	Error angle in y direction(')	Error angle in z direction(')
Fix error angle	RMS	0.8060	1.8441	0.1197
	STD	0.1001	0.2189	0.1180
Flexural deflection angle	RMS	—	1.0680	—
	STD	—	0.5962	—

5 Conclusions

Aiming at effects on transfer alignment to flexural deflection of wings, in this thesis modeling method of elastic mechanics is adopted to accurately establish mathematical modeling to flexure motion of wings. Compared to traditional Markov equivalent modeling method, this method could give out more real modeling parameters combined with actual application objects. On this basis, this thesis

establishes a filter model of “velocity + attitude” matching with transfer alignment, and carries out semi-physical simulation verification combined with ground demonstration POS of distributed POS. From the third section, after maneuver turning, estimated precision of x direction and y direction is very high, estimated error is within 3'; precision of z direction is slightly lower, but it’s also within 5'. This implies that the model established in this thesis could effectively estimate fix error angle and flexural deflection.

Simulation results show that utilizing the model proposed in this thesis, estimated value of attitude error angle between main and slave POS could be obtained precisely through Kalman filtering method.

References

[1] Wei L D, Xiang M S, Wu Y R. POS data using for motion compensation of airborne InSAR[J]. Remote sensing technology and application, 2007, 2: 013.

[2] Wang C M, Tan V B C, Zhang Y Y. Timoshenko beam model for vibration analysis of multi-walled carbon nanotubes[J]. Journal of Sound and Vibration, 2006, 294(4): 1060-1072.

[3] Kim J U, Renardy Y. Boundary control of the Timoshenko beam[J]. SIAM journal on control and optimization, 1987, 25(6): 1417-1429.

[4] Nelson H D. A finite rotating shaft element using Timoshenko beam theory[J]. Journal of Mechanical Design, 1980, 102(4): 793-803.

[5] Fang J C, Zhang Z, Gong X L. Modeling and simulation of transfer alignment for distributed POS[J]. Journal of Chinese Inertial Technology, 2012, 4: 002.

[6] Kain J E, Cloutier J R. Rapid transfer alignment for tactical weapon applications[C]//AIAA Guidance, Navigation and Control Conference. 1989: 1290-1300.

[7] Tekinalp O, Ozemre M. Artificial neural networks for transfer alignment and calibration of inertial navigation systems[J]. computing, 2001, 6: 7.